RD Status Report/RD39
19th November 2008

RD39 STATUS REPORT 2008

CERN RD39 Collaboration

X.Rouby[j], P. Anbinderis[m], T. Anbinderis[m], R. Bates[e], W. de Boer[h], E. Borchi[c], M. Bruzzi[c], S. Buontempo[k], C. Buttar[e], W. Chen[b], V. Cindro[i], V. Eremin[l], A. Furgeri[h], E. Gaubas[m], J. Härkönen[g], E. Heijne[a], I. Ilyashenko[l], V. Kalesinskas[m], M. Krause[h], Z. Li[b], P. Luukka[g], I. Mandic[i], D. Menichelli[c], M. Mikuz[i], O. Militaru[j], H. Moilanen[g], S. Mueller[h], T. Mäenpää[g],T.O. Niinikoski[a],V. O'Shea[e], S. Pagano[k], C. Parkes[e], K. Piotrzkowski[j], S. Pirollo[c], P. Pusa[f] J. Räisänen[f], E. Tuominen[g], E. Tuovinen[g], J. Vaitkus[m], E. Verbitskaya[l], S. Väyrynen[f], M. Zavrtanik[i]

[a]*CERN, CH-1211 Geneva, Switzerland*

[b]*Brookhaven National Laboratory, Upton, NY 11973-5000, USA*

[c]*Dipartimento di Energetica, Universitá di Firenze, I-50139 Firenze, Italy*

[e]*Department of Physics and Astronomy, University of Glasgow, Glasgow G12 8QQ, United Kingdom*

[f]*Accelerator Laboratory, University of Helsinki, 00014 University of Helsinki, Finland*

[g]*Helsinki Institute of Physics, 00014 University of Helsinki, Finland*

[h]*IEKP University of Karlsruhe, D-76128 Karlsruhe, Germany*

[i]*Jozef Stefan Institute, Experimental Particle Physics Department, 1001 Ljubljana, Slovenia*

[j]*Université Catholique de Louvain, FYNU, Louvain-la-Neuve, Belgique*

[l]*Ioffe Physico-Technical Institute, Russian Academy of Sciences, St.Petersburg 194021, Russia*

[m]*University of Vilnius, Institute of Materials Science and Applied Research, 2040 Vilnius, Lithuania*

CERN-LHCC-2008-019 / LHCC-SR-001
18/11/2008

Summary

CERN RD39 Collaboration is aiming for development of super-radiation hard cryogenic silicon detectors for applications of LHC experiments and their future upgrades. Radiation hardness up to 1×10^{16} n_{eq}/cm^2 is required in the future HEP experiments. The most important measure of the detector's radiation hardness is the Charge Collection Efficiency (CCE), which is affected by both the detector sensitive volume (depletion depth) and charge trapping by radiation-induced trapping centers. However, 1×10^{16} n_{eq}/cm^2 fluence is well beyond the radiation tolerance of even the most advanced semiconductor detectors fabricated by commonly adopted technologies. First, the full depletion voltage (V_{fd}) will be in the thousands of volts for a 300 μm thick Si detector operated at or near room temperature. Second, the charge carrier trapping will limit the charge collection depth to an effective range of 20 μm to 30 μm regardless of depletion depth. In order to maintain an acceptable CCE under Super LHC radiation environment, one has to solve both problems simultaneously.

The activities of RD39 Collaboration were focused in 2008 on concept of charge injected detector (CID). In a CID, the electric field is controlled by injected current, which is limited by the space charge. This leads to continuous electric field through the detector at any operating voltage regardless of the radiation fluence. The electric field distribution in CID is proportional to the square of the distance starting from the charge injection contact. According to the calculations with known electric field distribution one could expect more than two times higher CCE in CID compared with similar detector under reverse bias. Moderately low temperature and high concentration of deep levels are required in order to establish by charge injection the stable electric favorable for detector operation.

C-TCT tests on CID pad detectors and muon beam tests (at CERN H2) on CID micro strip detectors mounted to the CMS APV25 readout chips have shown very good CCE: for detectors irradiated to 3×10^{15} n_{eq}/cm^2, a CCE of over 70% (or > 15000 electrons) have been achieved by CID detectors, as compared to only 20% (or 5000 electrons) by detectors operated in the conventional reverse bias mode. Good tracking efficiency and position resolutions have also be obtained by CID detectors in the beam test.

1. Introduction

1. Introduction

For LHC upgrade, the SLHC, the expected radiation level will be 10 times higher, up to $1x10^{16}$ n_{eq}/cm^2 than the current LHC. In this case, in addition to the detector full depletion problem, the trapping problem is now one of the main limiting factors to CCE.
In our previous estimation for CCE and collected charge, we use the approximation of short-range particle (such alpha and red laser) generated charge sheet moving across the detector in the electric field [RD39 Status Report 2007]. While the physics principle remains true for these estimations, it is not accurate in absolute details of the case of MIP generated charges, which are the case for LHC/SLHC experiments. For simplicity, we will make the estimation of charge collection and CCE in a pad detector (non-segmented detector) in the case of MIP generated charges. For MIP, the generated charge density in a Si detector is Q_0/d. For a detector with a depletion depth of w, the charge that causes an induced current is Q_0*w/d. The induced current by an electron charge sheet of $Q_0/d\ \Delta x$ located at x is:

$$\Delta i(t,x) = Q_0 \cdot e^{-t/\tau_t^e} \cdot \frac{\Delta x}{d}\frac{1}{w} \cdot V_{dr}^e \tag{1}$$

where τ_t^e is trapping time constant of electrons, V_{dr}^e the drift velocity of electrons, which we assume is a constant for simplicity in a constant electric filed in the depletion region. The collected charge due to drift of electrons is:

$$Q_e = \int_0^w \int_0^{t_{dr}^e(x)} \Delta i(t,x)dt = \int_0^w \int_0^{t_{dr}^e(x)} Q_0 \cdot (\frac{dx}{d}) \cdot e^{-t/\tau_{t\,t}^e} \cdot \frac{1}{w} \cdot V_{dr}^e dt \tag{2}$$

Where $t_{dr}^e(x) = (w-x)/V_{dr}^e$, and $t_{dr}^e = w/V_{dr}^e$

Integrations of Eq. (2) give:

$$Q_e = Q_0 \cdot \frac{V_{dr}^e \tau_t^e}{d} \cdot [1 - \frac{V_{dr}^e \tau_t^e}{w} \cdot (1 - e^{-t_{dr}^e/\tau_t^e})] \tag{3}$$

We define $d_{CCEr}^e = V_{dr}^e \tau_t^e$ as the charge collection distance (or trapping distance) for electrons, and have:

$$Q_e = Q_0 \cdot \frac{d_{CCE}^e}{d} \cdot [1 - \frac{d_{CCE}^e}{w} \cdot (1 - e^{-t_{dr}^e/\tau_t^e})] \tag{4}$$

Similarly, the collected charge due to drift of holes is:

$$Q_h = Q_0 \cdot \frac{d_{CCE}^h}{d} \cdot [1 - \frac{d_{CCE}^h}{w} \cdot (1 - e^{-t_r^h/\tau_t^h})] \tag{5}$$

And the total collected charge for a planar Si detector is:

$$Q = \frac{Q_0}{d} \cdot \left\{ d^e_{CCE} \cdot [1 - \frac{\tau^e_t}{t^e_{dr}} \cdot (1 - e^{-t^e_{dr}/\tau^e_t})] + d^h_{CCE} \cdot [1 - \frac{\tau^h_t}{t^h_r} \cdot (1 - e^{-t^h_r/\tau^h_t})] \right\} \quad (6)$$

Some approximations:

$$Q \cong \begin{cases} \frac{Q_0}{2} \cdot \frac{w}{d} \cdot [(1 - \frac{1}{3}\frac{t^e_{dr}}{\tau^e_t}) + (1 - \frac{1}{3}\frac{t^h_{dr}}{\tau^h_t})] \quad (\text{low fluences, } \frac{\tau^e_t}{t^e_{dr}} >> 1) \\ \\ \frac{Q_0}{d} \cdot (d^e_{CCE} \cdot (1 - \frac{\tau^e_t}{t^e_{dr}}) + d^h_{CCE} \cdot (1 - \frac{\tau^h_t}{t^h_r})] \cong Q_0 \cdot \frac{d^e_{CCE} + d^h_{CCE}}{d} \quad (\text{high fluences, } \frac{\tau^e_t}{t^e_{dr}} << 1) \end{cases} \quad (7)$$

Expressing Q_0 in number of electrons $Q_0 = 80 e's/\mu m \cdot d \ (in \ \mu m)$, we have:

$$Q \cong \begin{cases} 40w \cdot [(1 - \frac{1}{3}\frac{t^e_{dr}}{\tau^e_t}) + (1 - \frac{1}{3}\frac{t^h_{dr}}{\tau^h_t})] \quad (\#\text{ of e's, low fluences, } \frac{\tau^e_t}{t^e_{dr}} >> 1) \\ \\ 80 \cdot [d^e_{CCE} \cdot (1 - \frac{\tau^e_t}{t^e_{dr}}) + d^h_{CCE} \cdot (1 - \frac{\tau^h_t}{t^h_r})] \cong 80 \cdot (d^e_{CCE} + d^h_{CCE}) \quad (\#\text{ of e's, high fluences, } \frac{\tau^e_t}{t^e_{dr}} << 1) \end{cases} \quad (8)$$

Assuming $\tau^e_t = \tau^h_t = \tau_t$, and in very high E-filed ($V^e_{dr} \cong V^h_{dr} \cong V_s$, $t^e_{dr} \cong t^h_{dr} = t_{dr} \cong w/V_s$, and $d^e_{CCE} \cong d^h_{CCE} = d_{CCE} \cong V_s \tau_t$):

$$Q \cong \begin{cases} 80w \cdot (1 - \frac{1}{3}\frac{t_{dr}}{\tau_t}) \quad (\#\text{ of e's, low fluences, } \frac{\tau_t}{t_{dr}} >> 1, \text{and high field}) \\ \\ 160 \cdot d_{CCE} \quad (\#\text{ of e's, high fluences, } \frac{\tau^e_t}{t^e_{dr}} << 1, \text{and high field}) \end{cases} \quad (9)$$

In the case of low fluence (<2x10^{15} n_{eq}/cm^2), the detector depletion depth w is still an important factor in the collected charge, which depends on the bias voltage:

$$w = \sqrt{\frac{2\varepsilon\varepsilon_0 V}{eN_{eff}}} \quad (10)$$

where e is the electronic charge, ε the permittivity of Si, ε_0 the permittivity of vacuum, V the bias voltage, and N_{eff} the effective space charge density.

For high fluences (>2x10^{15} n_{eq}/cm^2), we found that collected charge only depends on the charge collection distance that is affected only by trapping. The electric field only has to be high enough to ensure that the depletion depth w is larger than the charge collection distance d_{CCE}, which is about 20 μm at 1x10^{16} n_{eq}/cm^2.

The trapping (τ_t) and de-trapping (τ_d) time constants for a trap level can be defined by:

$$\begin{cases} \tau_t = \dfrac{1}{\sigma v_{th} N_t} \\ \tau_d = \dfrac{1}{\sigma v_{th} N_C e^{-E_t/kT}} \end{cases} \quad (11)$$

where σ is the capture cross section of the trap, v_{th} is the thermal velocity of charge carriers, N_T is the concentration of traps, N_C the electric state density in the conduction band, and E_t the trap energy level in the band gap.

The trapping time constant is nearly independent on temperature (or weak dependence on T). However, it depends strongly on the radiation fluence Φ_n. At a fluence of 10^{16} n_{eq} /cm^2, the trapping time can be as short as 0.2 ns [1-2], which will give a collected charge of about 3200 e's for MIP.

The estimation done above again is for a pad detector with no segmentation, and a simple weighting field. For a real segmented detector with complicated weighting field, the charges might not be the same, but they should be in the same order of magnitude.

As we mentioned before, for extremely high fluence (10^{16} n/cm^2) in LHC upgrade environment, the trapping term can be significant and affect the CCE greatly. The approach of RD39 to overcome the fundamental trapping problem at very high fluencies is to modify the CCE_t by filling the traps so that thy are neutral (or inactive) for further trapping of free carriers generated by particles. The key of our approach is to use the charge-injection-detector concept that can achieve a nearly full depletion at any fluence and in the mean time to partially fill the traps that are responsible for charge trapping. In doing so, we can improve CCE by simultaneously manipulating the electric field and partially removing trapping through current injection.

2. Characterization of Charge Injected Detectors (CID) by Cryogenic Transient Current Technique (C-TCT).

The RD39 Collaboration has constructed Cryogenic Transient Current Technique (C-TCT) measurement setup, which is capable to operate below liquid nitrogen temperatures [3]. The C-TCT is an effective research tool to study heavily irradiated silicon detectors. The TCT measurement is based on the detection of the dominant type of charge carrier, electron or hole, which drifts across the whole detector thickness after being excited by a photon. This is achieved by illuminating (i.e. $n^+/p^-/p^+$ device) the front (n^+ implant) or back (p^+ implant) side of the detector with a red laser, whose light creates electron-hole pairs close to the device surface. When the front-side of the detector is illuminated, the electrons move only a few microns (small signal) and are gathered to the n^+-electrode so fast that the signal is damped by the rise-time of the data acquisition electronics and therefore the measured signal is mainly coming from the holes that travel a longer distance through the silicon bulk. By analyzing the transient, it is possible to extract the full depletion voltage, effective trapping time, electric field distribution and the sign of the space charge in the silicon bulk [4,5]. Furthermore, the CCE can be determined if the detector is illuminated by sub band gap infrared light, which provides homogenous generation of electron hole pairs through the entire bulk of silicon and

therefore simulate minimum ionizing particles [6]. The CCE can be obtained by comparing the signal from irradiated detector with signal measured from non-irradiated sample. An example of such measurement is shown in Figure 1.

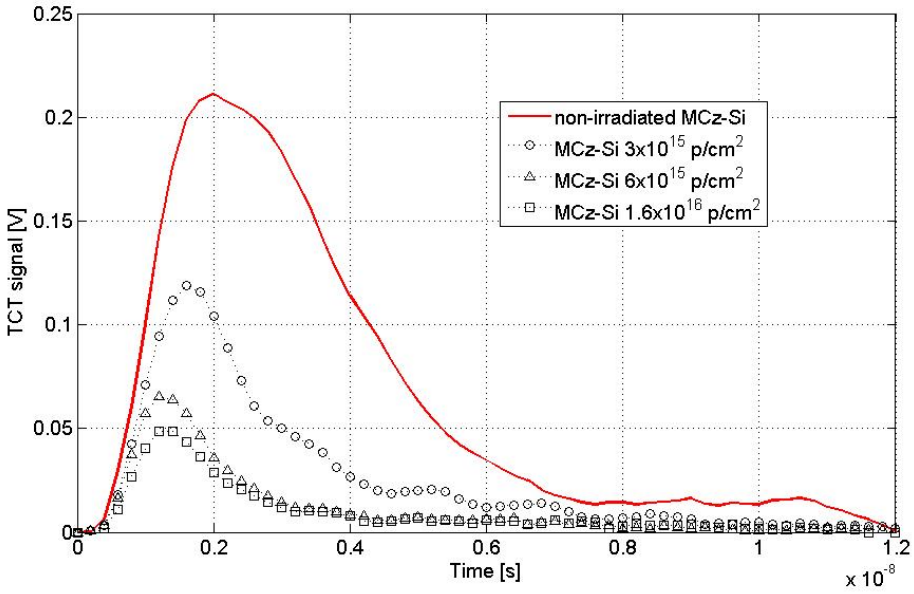

Figure 1. IR signals of 24 GeV/c proton irradiated MCz-Si detectors with respect of non-irradiated reverse biased reference detector. The detectors are 300μm thick $p^+/n^-/n^+$ structures. The reverse bias of detectors is 500V and the measurements have been performed at -50^{0}C.

Figures 2-5 show CID detector signals compared with same device under the reverse bias. The detectors have been irradiated with 24 GeV/c proton beam up to Super-LHC fluencies 6×10^{16} p/ cm^2 and 1.6×10^{16} p/cm^2. The pad detectors have been processed on n and p-type MCz-Si wafers at Helsinki University of Technology Microelectronics Centre (Micronova) [7]. The starting material of the detectors was 100mm diameter double-side-polished 300±2 μm-thick <100> n and p-type Magnetic Czochralski silicon (MCz-Si) wafers. The nominal resistivity, measured by the four point probe method, of the wafers is 900-1100 Ωcm for n-type wafers and 3kΩcm for p-type wafers, respectively.

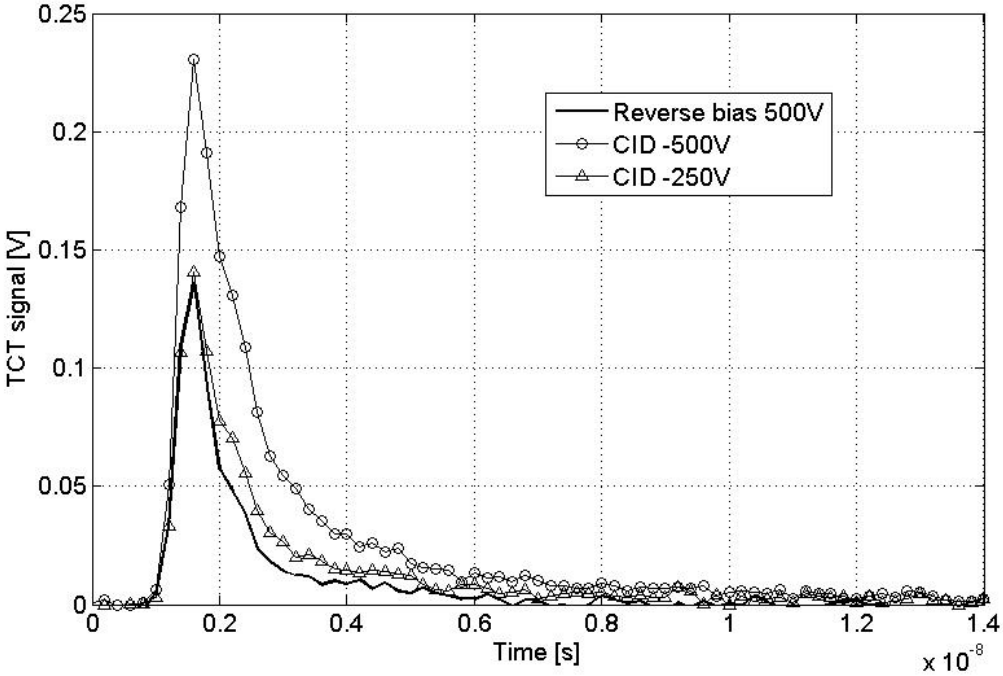

Figure 2. Infrared laser response of detector made on n-type MCz-Si wafer ($p^+/n^-/n^+$ structure). The irradiation fluence is 1.6×10^{16} p/ cm^2. The measurement temperature is 220K.

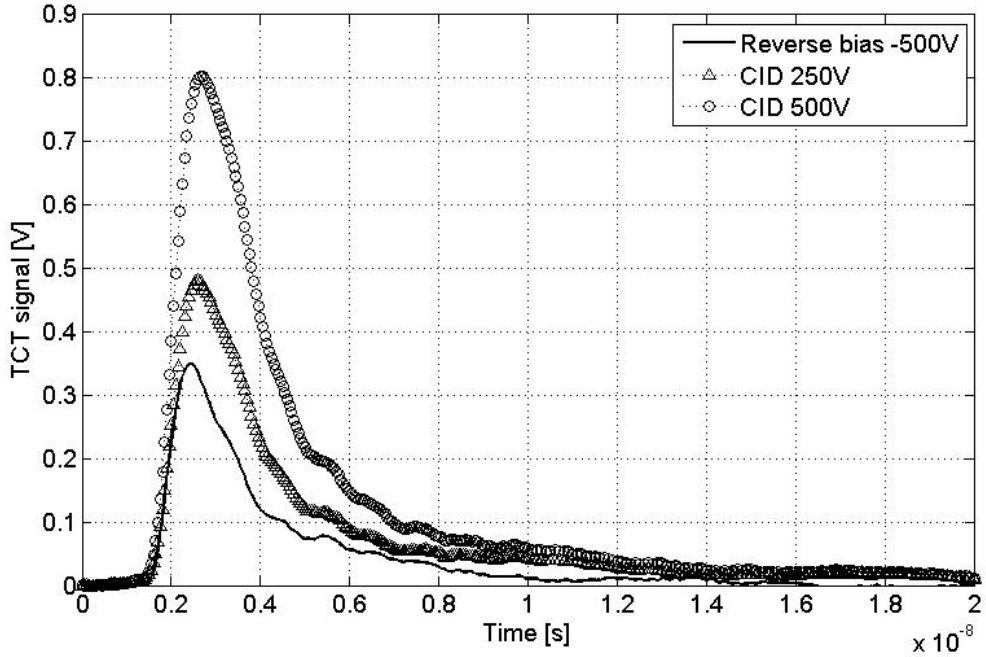

Figure 3. Infrared laser response of detector made on p-type MCz-Si ($n^+/p^-/p^+$ structure). The irradiation fluence is 6.0×10^{15} p/ cm^2. The measurement temperature is 220K.

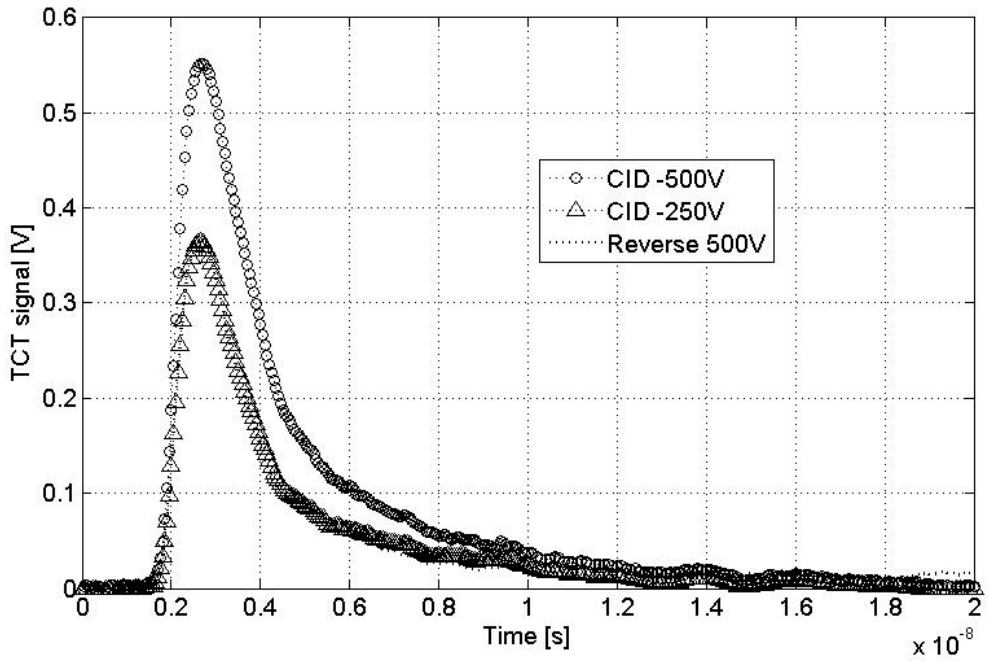

Figure 4. Infrared laser response of detector made on n-type MCz-Si wafer ($p^+/n^-/n^+$ structure). The irradiation fluence is 1×10^{16} n_{eq}/ cm^2. The measurement temperature is 220K.

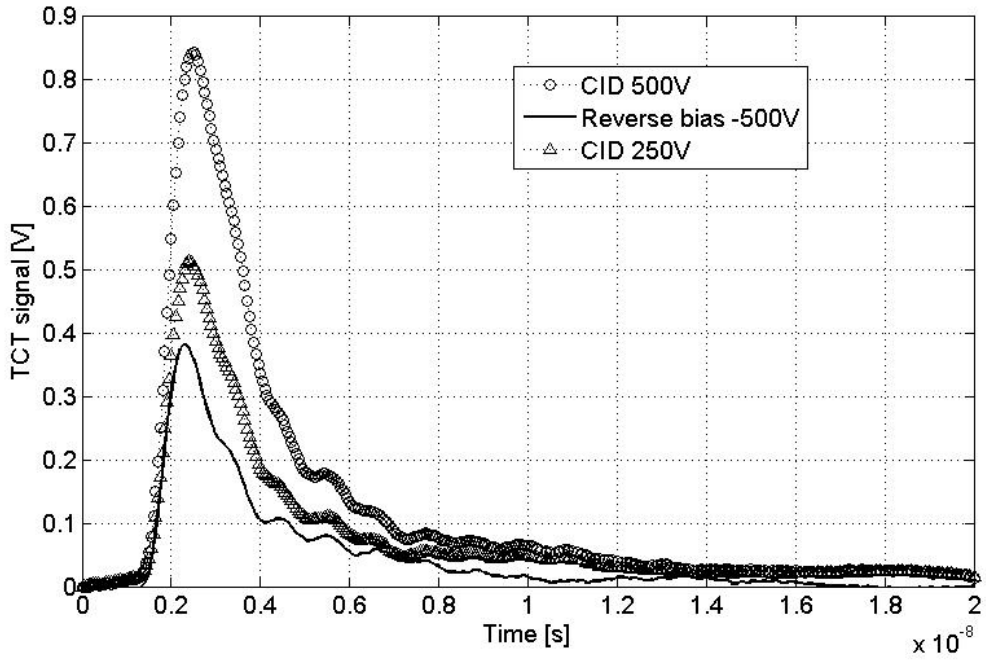

Figure 5. Infrared laser response of detector made on p-type MCz-Si ($n^+/p^-/p^+$ structure). The irradiation fluence is 6.0×10^{15} p/ cm^2. The measurement temperature is 220K. The IR

laser has been tuned to output higher excitation than during the measurement shown in Fig 2.

It can be seen in figures 2-5 that the signal in CID mode is higher than under reverse bias regardless of type of detector or fluence. In n-type sensors, the signal is identical in 1×10^{16} n_{eq}/ cm^2 irradiated sample when detector is biased in CID mode with -250V and when the detector is reverse biased with 500V. With -500V under CID mode, the collected charge is significantly higher. In $n^+/p^-/p^+$ detector, the collected charge is essentially higher already with 250V CID mode than with -500V reverse bias at both fluencies.

During the QV measurements the current in detectors bias circuit was also recorded. The current voltage (IV) characteristics of 1×10^{16} 1 MeV neutron equivalent / cm^2 irradiated pad detector are shown in figure 6.

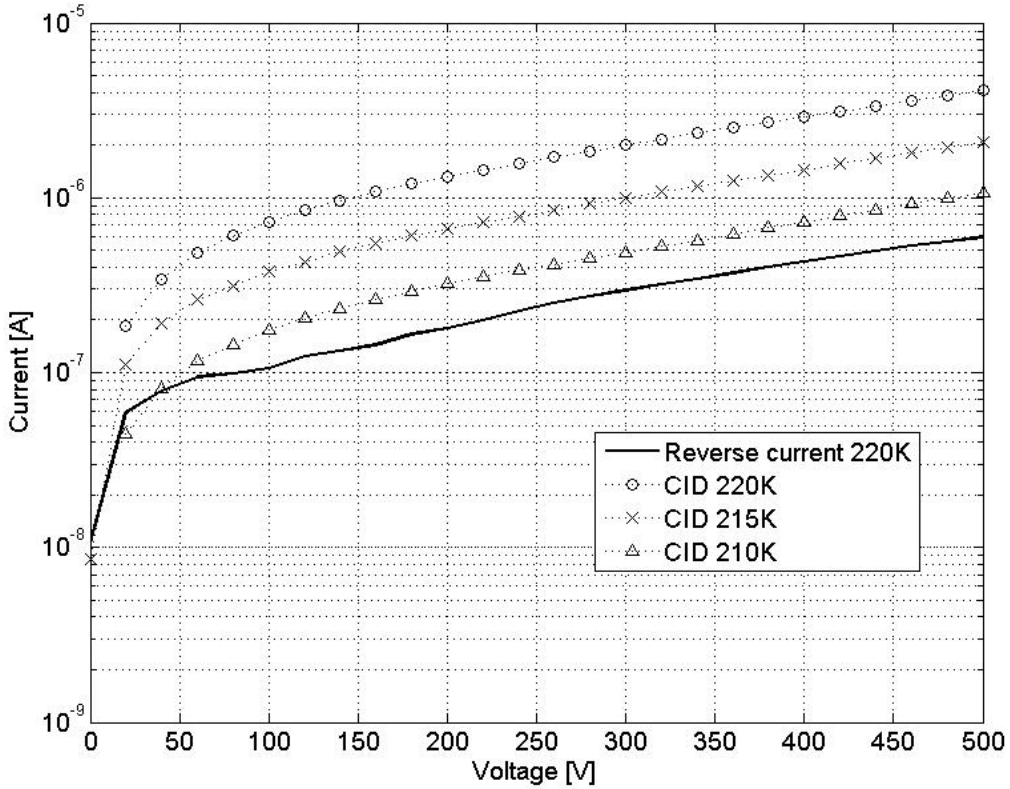

Figure 6. 1×10^{16} 1 MeV n_{eq}/ cm^2 irradiated pad detector. The detector is the same device, which CCE has been shown in figure 2. The size of the sample is 0.25 cm^2.

It can be seen in figure 6. that the forward current of heavily irradiated detector is order of few microampers in the temperature range 220-210K. The IV curves have same shape under current injection and reverse bias both.
The CCE measurements with C-TCT setup are summarized in Figure 7.

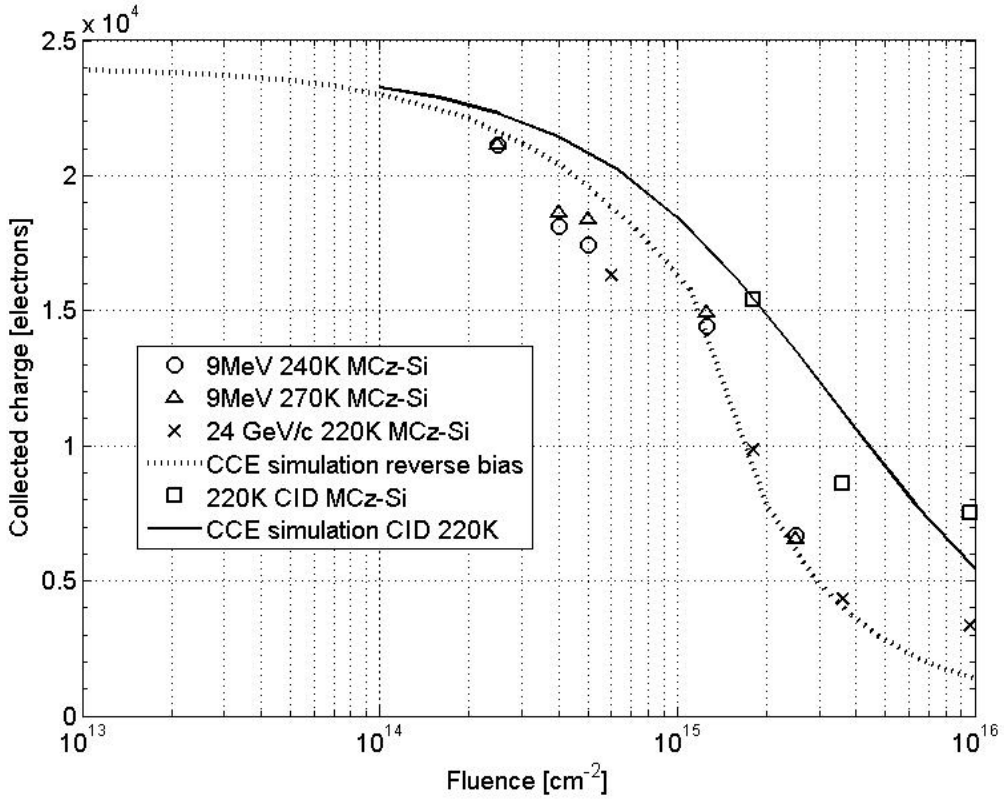

Figure 7. Experimental data points and simulation of CID and reverse biased detectors. The simulation assumes 220K temperature and 500V operating voltage for reverse biased and CID detectors both.

The experimental data points in Figure 7 are compared with simulations shown with dashed lines. The simulation of CCE assumes linear trapping, i.e. at fluencies 1×10^{14} n_{eq}/cm^2,1×10^{15} n_{eq}/cm^2 and 1×10^{16} n_{eq}/cm^2 the values for τ_t are 25ns, 2.5ns and 0.25ns, respectively [1,2]. The simulation and measurements have done with 500V reverse bias and taking in to the account the carrier mobility temperature dependence. As it can be seen, the CCE starts to decrease rapidly after about 7×10^{14} n_{eq}/cm^2 fluence. This is the fluence where the V_{fd} of 300µm thick MCz-Si detectors reaches the 500V and if the irradiation continues the detector will not be fully depleted anymore.

3. Test beam measurements on CID detectors.

In order to demonstrate that new detector concept, such as the CID, is suitable for large scale tracker systems, it is necessary to perform extensive tests on full detector systems, i.e. segmented devices with their readout electronics. The CCE is partly determined by the electric field distribution in silicon. In irradiated silicon, the electric field distribution is complicated and contains e.g. so called Double Junction (DJ) [8]. Additionally, the electric field distribution depends on the geometry, i.e. the segmentation

of the sensor. This effect is called weighting field and it means that particle generated charge induces most charge in the segmented electrode when it is close to it, and not uniformly through the entire volume like in a diode [9,10]. Thus, higher charge collection is expected in segmented detectors than in diodes used in most radiation hardness studies this far. Additionally, the CCE is greatly influenced whether the SCSI has been taken place in the silicon bulk. Despite of extensive studies during the past years, the SCSI is poorly understood in potentially radiation hard silicon materials [11]. A degradation of cluster resolution after assumed type inversion fluence would be an evidence of SCSI. Because of these reasons, it is mandatory to perform radiation hardness investigations between CID and standard detector operation mode with a beam telescope providing reference tracks.

The SiBT measures the tracks of energetic particles hence providing a reference measurement for a detector under investigation [12]. The telescope was completely reconstructed in 2007 together with CMS groups from Fermilab, University of Karslruhe and University of Rochester. The read-out electronics and data acquisition (DAQ) of the upgraded SiBT is based on the actual CMS hardware and software operating at LHC compatible rate. The telescope contains 8 reference detector planes in ±45 degree orientation and has two slots for the devices to be tested. The reference sensors are produced by Hamamatsu K.K. and they are originally designed for the Fermilab D0 Run IIb. The interpolated position resolution of the reconstructed SiBT is 9 μm, it has a signal to noise ratio (S/N) of 25 and an active area of 4 x 4 cm^2. The telescope can be cooled down to -20°C temperature, which is mandatory when studying highly irradiated sensors. In order to measure full size CID detector modules at temperatures down to -50^0C, an additional cold box was designed and constructed. The cold box consists of three Peltier elements having total cooling power 350W and heat removal system. The cold finger and its schematical layout are shown in Figure 8.

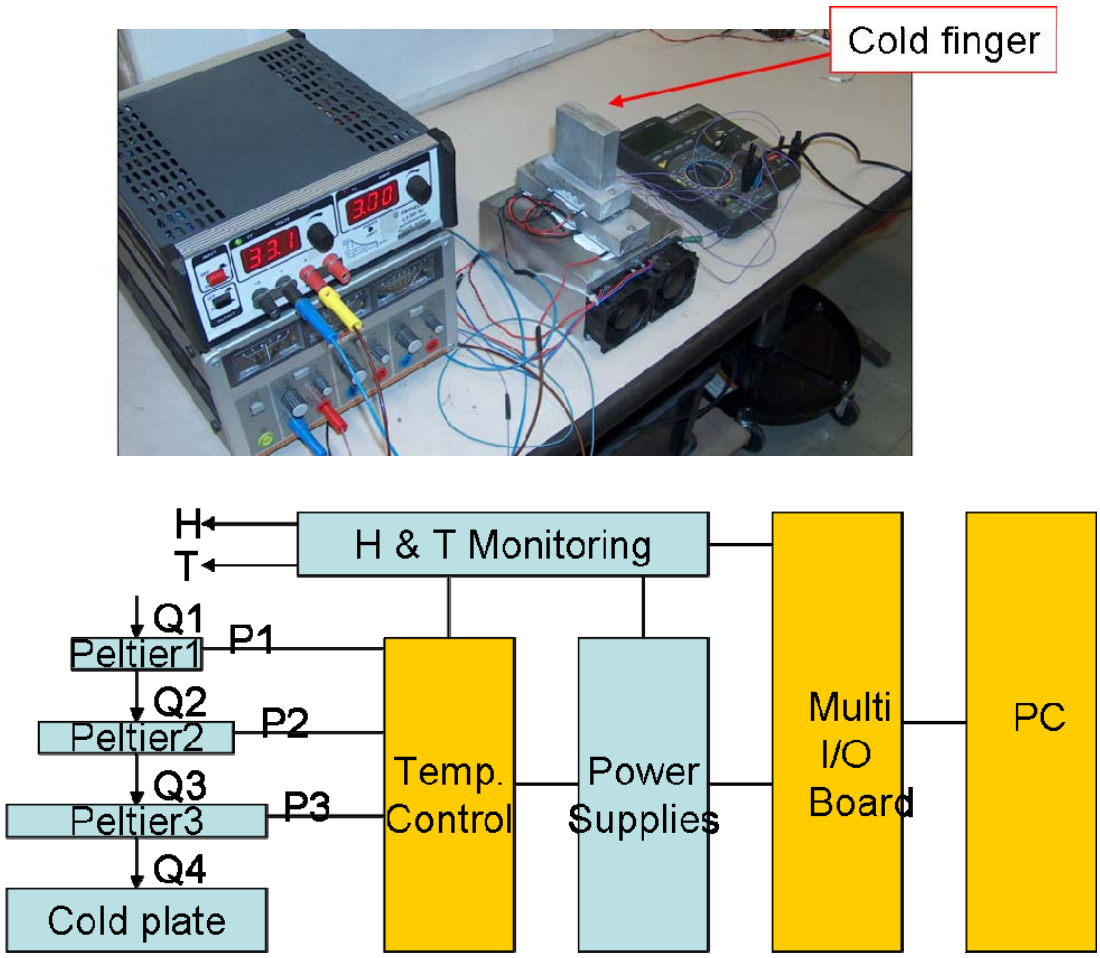

Figure 8. Schematical layout and cold finger that were used for the CID detector beam tests in summer 2008.

An overview of the experimental setup is shown in Figure 9.

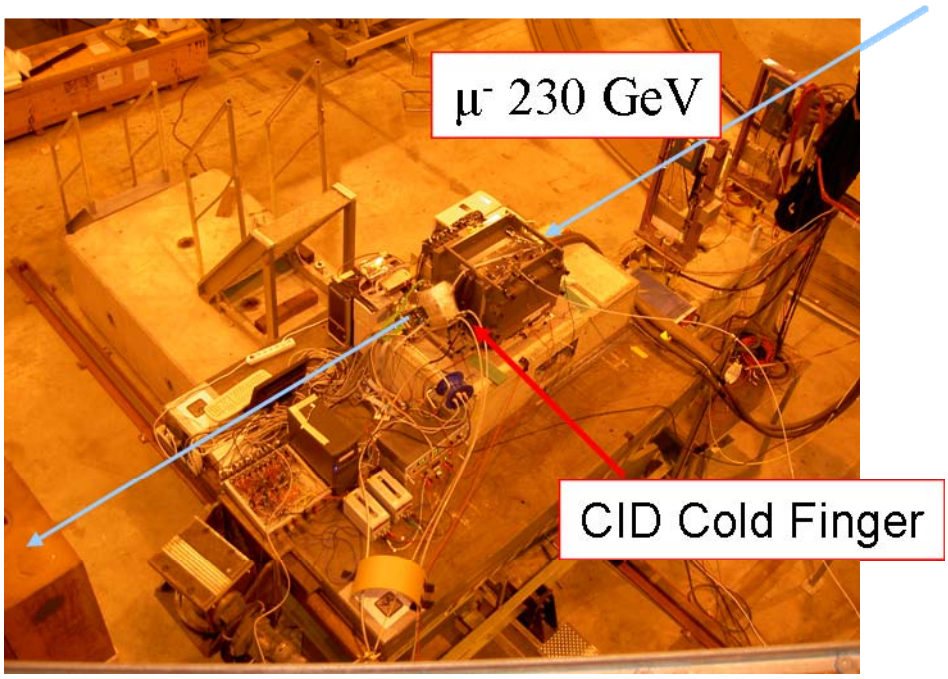

Figure 9. SiBT installed at CERN H2 experimental area.

The MCz-Si detector used in CID study was processed with a simple six mask level process at the Helsinki University of Technology Centre for Micro and Nanotechnology (MINFAB) facility. The starting material was 4" n-type wafers with a thickness of 300±2μm and <100> crystal orientation grown with the MCz method by Okmetic Ltd., Finland.The large area strip detectors had 768 channels and an area of 4.0×4.0 cm^2. In the detector design the strip pitch was 50 μm, strip width 10 μm and the strip length 3.9 cm. The detector was irradiated with 26 MeV protons (Universität Karlsruhe) to the fluences of 3×10^{15} 1 MeV n_{eq}/cm^2 and after cooling bonded to an APV25 read-out hybrid. During the operation, the SiBT was capable to record about 25000 events in 20 min with modified CMS DAQ software. The results presented in this content are based on tracking, i.e. only events that were seen with all reference telescope planes are included to the analysis. The details of the off-line data analysis are reported in references [12].

The CID detector was measured in intense muon beam at different temperatures and bias voltages. The minimum temperature reached during the operation was -53^0C. Figure 10 shows the signals of detector irradiated 3×10^{15} 1 MeV n_{eq}/cm^2 in CID mode and under reverse bias.

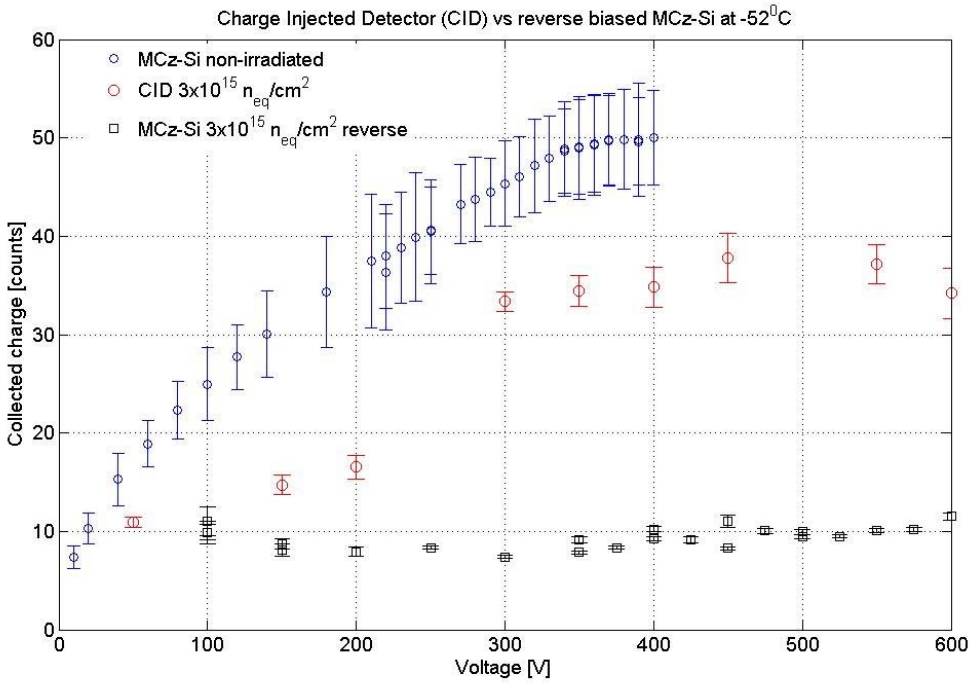

Figure 10. Collected charge in terms of arbitrary units (ADC counts) as function of voltage for CID, same detector with reverse bias and for a non-irradiated MCz-Si reference detector. The measurement of non-irradiated detector has been made at -20^{0}C.

It can be seen in Figure 10 that the signal of a non-irradiated MCz-Si reference detector saturates at about 330V for about 50 ADC counts value. The 330V full depletion voltage is very much expected according to earlier studies performed on n-type MCz-Si by various groups [13]. The CID detector signal reaches values about 35 after 300 volts. The same sensor under reverse bias at the same temperature -53^{0}C shows about 10 ADC value for the signal, i.e. more than three time less.
The noise recorded by the read-out and DAQ as function of bias voltage of CID detector at various temperatures is shownin Figure 11.

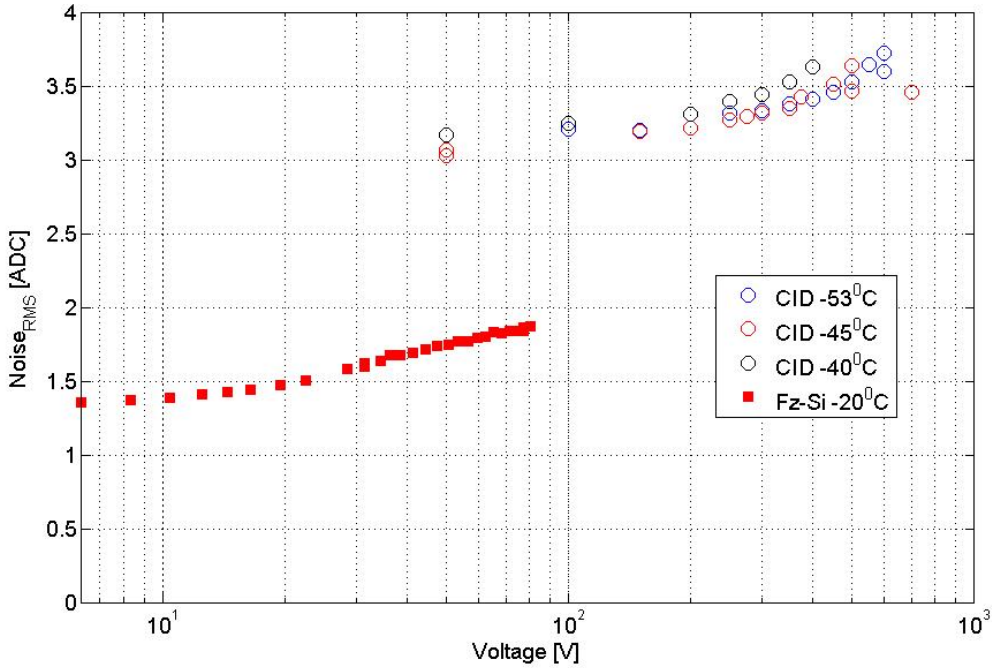

Figure 11. Noise of CID detectors between -40°C and -53^{0}C. The closed red symbols are for non-irradiated reference sensor made of high resistivity Fz-Si. The V_{fd} of Fz-Si sensor is less than 10V.

The noise of CID detector reaches values 3.5-3.8 at the highest voltages. This would result in signal-to-noise (S/N) ratio of about 10 after 3×10^{15} 1 MeV n_{eq}/cm^2 irradiation. The noise recorded from reference Fz-Si module is less than 1.5 at it's V_{fd}.

References

[1] H.W. Kraner et al., Nucl. Instr. and Meth. A326 (1993) 350-356
[2] G. Kramberger et al, Nucl. Instr. and Meth. **A481** (2002) 297.
[3] J. Härkönen et al., Nucl. Instr. and Meth **A581** (2007) 347.
[4] V. Eremin, Nucl. Instr. and Meth **A372** (1996) 388-398.
[5] V. Eremin et al., Nucl. Instr. And Meth, **A372** (1996) 188.
[6] B. Dezillie et al., Nucl. Instr. and Meth. A452 (2000) 440.
[7] J. Härkönen et al., Nucl. Instr. and Meth **A579** (2007) 648.
[8] E. Verbitskaya et al, Nucl. Instr. and Meth. **A 514** (2000) 47.
[9] T. J. Brodbeck, et al., Nucl. Instr. and Meth A455 (2000) 645.
[10] G. Kramberger, et al., Nucl. Instr. and Meth A476 (2002) 645.
[11] M. Bruzzi et al.; Radiation-Hard Semiconductor Detectors for Super LHC; Nucl. Instr. and Meth. **A541** (2005) 189-201.
[12] T. Maenpaa et al., Nucl. Instr. and Meth **A593** (2008) 523-529.
[13] RD50 Collaboration, Status Reports 2003-2007.